HHS Public Access

Author manuscript

J Phys Chem B. Author manuscript; available in PMC 2017 March 17.

Published in final edited form as:

J Phys Chem B. 2016 March 17; 120(10): 2761–2770. doi:10.1021/acs.jpcb.5b10165.

Thickness Mismatch of Coexisting Liquid Phases in Non-Canonical Lipid Bilayers

Joan V. Bleecker[†], **Phillip A. Cox**[†], **Rami N. Foster**[‡], **Jonathan P. Litz**[†], **Matthew C. Blosser**[†], **David G. Castner**[‡,∥], and **Sarah L. Keller**[†,*]

[†]Department of Chemistry, University of Washington, Seattle, Washington 98195, United States

[‡]Department of Chemical Engineering, University of Washington, Seattle, Washington 98195, United States

[∥]Department of Bioengineering, University of Washington, Seattle, Washington 98195, United States

Abstract

Lipid composition dictates membrane thickness, which in turn can influence membrane protein activity. Lipid composition also determines whether a membrane demixes into coexisting liquid-crystalline phases. Previous direct measurements of demixed lipid membranes have always found a liquid-ordered phase that is thicker than the liquid-disordered phase. Here we investigated non-canonical ternary lipid mixtures designed to produce bilayers with thicker disordered phases than ordered phases. The membranes were comprised of short, saturated (ordered) lipids; long, unsaturated (disordered) lipids; and cholesterol. We found that few of these systems yield coexisting liquid phases above 10 °C. For membranes that do demix into two liquid phases, we measured the thickness mismatch between the phases by atomic force microscopy and found that not one of the systems yields thicker disordered than ordered phases under standard experimental conditions. We found no monotonic relationship between demixing temperatures of these ternary systems and either estimated thickness mismatches between the liquid phases or the physical parameters of single-component membranes comprised of the individual lipids. These results highlight the robustness of a membrane's liquid-ordered phase to be thicker than the liquid-disordered phase, regardless of the membrane's lipid composition.

INTRODUCTION

The activity of membrane proteins can vary dramatically with local lipid composition.[1–2] Because lipid composition dictates many physical properties of a membrane, including

[*]**Corresponding Author**. slkeller@chem.washington.edu.

ASSOCIATED CONTENT

Supporting Information. Molecular structures and further methods are described in the Supporting Information, as are detailed data for membranes of 40/40/20 18:1-PC/16:0-PC/chol and for membranes of each system in Table 2. The Supporting Information is available free of charge via the Internet at http://pubs.acs.org.

The following files are available free of charge: Supporting Information (PDF)

Author Contributions

The manuscript was written through contributions of all authors. All authors have given approval to the final version of the manuscript.

thickness, lateral pressure, order, and elasticity,[3] isolation of the relationship between an individual physical parameter and protein activity is difficult. This difficulty is exacerbated when the protein explores different regions of the membrane with distinct compositions. Here we study the relationship between composition and membrane thickness in model membranes with micron-scale heterogeneities. Nanoscopic heterogeneities in cell membrane thickness have been proposed to be a key parameter in membrane trafficking.[4–5]

For a single-component lipid bilayer, membrane thickness is positively correlated with both the NMR order parameter of the lipid's acyl tail and the temperature at which the lipid melts from a gel phase to a liquid crystalline phase (T_{melt}).[6–7] All three of these parameters increase when the length or degree of saturation of the lipid tails is increased.[6–7] However, when there is a simultaneous increase in lipid tail length and decrease in lipid tail saturation, the correlation between membrane thickness, lipid order, and T_{melt} breaks down. Namely, single-component membranes comprised of monounsaturated phosphatidylcholine (PC)-lipids are thicker than membranes composed of saturated PC-lipids containing two fewer carbons per tail, despite the fact that the monounsaturated lipids are less ordered and have a lower T_{melt} than the saturated lipids.[6, 8–10]

Some ternary membranes comprised of a high-T_{melt} lipid, a low-T_{melt} lipid, and cholesterol (chol) demix below a threshold temperature (T_{mix}) into micron-scale regions of coexisting liquid phases.[11] The resulting phases are termed the liquid-ordered (Lo) and liquid-disordered (Ld) phases in reference to the lipid tail order within each phase.[12] A schematic of our experimental setup is given in Figure 1. The giant unilamellar vesicles (GUVs) contain a fluorescently labeled lipid that partitions into the Ld phase, making it brighter than the Lo phase.[13–15] To measure the thickness differences of the Lo and Ld phases, we deposited phase-separated vesicles on mica (Fig. 1, a3). The vesicles ruptured to form isolated supported lipid bilayers (Fig. 1, a4). We scanned the supported bilayers with atomic force microscopy to measure thickness differences. Our procedure is described fully in the Materials and Methods section.

An example of a GUV before and after rupture is shown in Figure 1b. The center image is a fluorescence micrograph of a phase-separated vesicle comprised of 18:1-PC/16:0-PC/cholesterol/Texas Red DHPE (40/40/20/0.8 mol/mol) at room temperature resting on a mica substrate. The Lo phase is difficult to distinguish from the background, so a schematic of the vesicle is provided to the left. The image on the right shows the isolated supported lipid bilayer formed after the vesicle ruptures. Canonically, the Lo phase, which is enriched in saturated low-T_{melt} lipids, is thicker than the Ld phase.[16]

Here we examine a series of non-canonical ternary systems composed of short-tailed ordered lipids and long-tailed disordered lipids. In particular, we study systems in which a single-component liquid membrane comprised of the disordered lipid is *thicker* than a single-component liquid membrane comprised of the ordered lipid. Table 1 lists the lipids in the ternary systems we investigate and the previously reported thickness differences between the corresponding single-component membranes in liquid phases[9–10]. Because the Ld phase is enriched in low-T_{melt} lipids, we hypothesized that some of the ternary systems in Table 1 would be good candidates for producing membranes with thicker Ld than Lo phases. Table 1

also lists estimates of thickness differences between Lo and Ld phases in the ternary systems.[10, 17–18] These estimates shift thickness differences by up to ~4 Å because they account for greater extension in the acyl chains of lipids in the ordered phase. Uncertainties in the estimates are at least 1 Å. These estimates predict at least one case of a thicker Ld than Lo phase. At minimum, the estimates in Table 1 illustrate the challenges of accurately calculating thickness differences between Lo and Ld phases using the paucity of currently available data.

Our motivation to study noncanonical membranes derives from recent literature in both physical chemistry and biophysics. Within the limited set of previous reports on thickness mismatch between Lo and Ld phases, there are no direct observations of a thicker Ld phase.[19–31] By producing membranes from unusual lipid mixtures that complement the canonical mixtures used in previous reports, we seek to provide a broader set of model systems for future studies on thickness-modulated protein activity and to constrain computational models that incorporate thickness mismatches between the Lo and Ld phases.[32–34] In addition, we seek to understand previously reported indirect results consistent with a thicker Ld phase. In that work, the authors interpreted changes in fluorescence signals as evidence that mutants of perfringolysin O of different lengths partition into different liquid phases of a model membrane.[35] The membrane used was a quaternary mixture that does not produce micron-scale liquid domains.

We narrowed our systems to those that are readily replicable, free of gel phase, and amenable to study by both fluorescence microscopy and room-temperature AFM. These constraints translate into four specific criteria. (1) To maximize reproducibility, we used lipids with at most one degree of unsaturation in each acyl chain, thereby minimizing the potential for photo-oxidation.[36–39] (2) To visualize the Lo and Ld phases by fluorescence microscopy, we chose membranes that demix into domains that are > 1 μm (larger than the diffraction limit of visible light). (3) To assess membrane thickness via room-temperature AFM, we examined vesicles that demix above room temperature. (4) To avoid preferential interactions between the AFM tip and different lipid moities, we used only lipids with the same headgroup (PC) and the same linkages (glycerol-ester).

We determined if each system is capable of liquid-liquid phase separation by fluorescence microscopy. For those membranes that demix into coexisting liquid phases above room temperature, we measured the thickness difference between the two phases by atomic force microscopy (AFM). Our results below show the robustness of a thicker Lo than Ld phase in membranes composed of widely accessible PC-lipids.

RESULTS

We produced three-component GUVs by mixing cholesterol with the pairs of lipids listed in each of the eight rows of Table 1. Structures of all lipids appear in the Supporting Information (Fig. S1). We used fluorescence microscopy to determine whether the resulting vesicles exhibited liquid-liquid phase separation in the temperature range of 10–50 °C. We plot our results on Gibbs phase triangles (Fig. 2). Of these eight systems, only two demix

into coexisting liquid phases above 25 °C (Fig. 2a), and two others exhibit coexisting liquid phases below 25 °C (Fig. 2b).

As expected, we find that the dye-labeled lipid (Texas Red DHPE) preferentially partitions to the Ld phase of the model membranes in Fig. 2a and 2b. Specifically, we observe larger area fractions of brightly-labeled membrane within vesicles made from lipid ratios with significant fractions of low-T_{melt} lipids (namely that fall to the left side of the two-phase coexistence regions in Fig. 2a and 2b). This result is consistent with observations of the same dye preferentially partitioning to the Ld phase in other lipid systems.[14, 40]

Three systems (Fig. 2c) do not separate into coexisting liquid phases, but instead exhibit gel-liquid coexistence. It is necessary to probe only a few compositions in order to determine that no macroscopic liquid-liquid phase coexistence occurs in these systems because any such coexistence would appear at the upper boundary of the gel-liquid region.[13, 41–46] The system consisting of 22:1-PC/16:0-PC/cholesterol (Fig. 2d) also does not exhibit liquid-liquid coexistence except in the case of intentional photo-oxidation, which is explicitly avoided elsewhere in our experiments, as outlined in the Materials and Methods section. Photo-oxidation, which typically raises T_{mix},[36, 38–39, 47] produces coexisting liquid phases at the composition marked with the colored circle in Fig. 2d.

In Figure 3 panels a–d, we quantify the relationship between the demixing temperature of the ternary systems and the physical properties of single-component bilayers. Specifically, we graph the highest system T_{mix} versus the difference in the number of carbons in the two PC-lipid tails (Fig. 3a), the highest lipid T_{melt} (Fig. 3b), the difference in thicknesses of the single-component liquid membranes (Fig. 3c), and the difference in T_{melt} of the single-component membranes (Fig. 3d). We find that there is no monotonic relationship between the highest T_{mix} of the ternary system and any of these single-component system parameters. Similarly, Fig. 3e shows that there is no monotonic relationship between the highest T_{mix} of the ternary system and the estimated thickness difference between the Lo and Ld phases in the ternary membranes investigated. The absence of clear correlation in any panel in Fig. 3 demonstrates the difficulty of predicting T_{mix} of ternary mixtures from the physical properties of the component lipids alone, or from estimated thickness differences between the Lo and Ld phases.

We also determined the thickness mismatch between the ordered and disordered phases in membranes exhibiting liquid-liquid phase coexistence above 25°C (Table 2). For the two systems in Fig. 2a, we assigned measured thicknesses to the Lo and Ld phases by comparing the Lo:Ld area ratios in fluorescence microscopy to the thick:thin area ratios in AFM for a population of vesicles. In these cases, we examined two different molar ratios per system: one rich in the Lo phase and the other rich in the Ld phase, for a total of four molar ratios.

To verify that the rupturing process does not change phase behavior, we measured the Lo:Ld area ratios both of free floating GUVs and of the resulting supported lipid bilayers. We found no significant change in area ratio. Values appear in the Materials and Methods section.

Next, we scanned the topography of individual supported lipid bilayers by AFM and measured the thick:thin area ratio and the thickness difference between the two phases. We determined that all four molar ratios described above produce membranes with thicker Lo phases than Ld phases. Fluorescence micrographs and AFM scans of bilayers comprised of 20/40/40 mol% 4Me-16:0-PC/13:0-PC/cholesterol appear in Fig. 4a–c. AFM data and height values are compiled in Tables S2–S6.

We found that GUVs comprised of 20/55/25 mol% 22:1-PC/16:0-PC/cholesterol phase separate only upon exposure to light. To enable intense light exposure to bilayers within the AFM apparatus, we moved from the original AFM setup to an AFM coupled to a fluorescence light source. The coupled microscope had the added advantage of allowing us to directly compare the Lo and Ld phases in fluorescence microscopy with the thicker and thinner phases in AFM (Fig. 4d,e). We found that the Ld phase was thicker than the Lo phase in this photo-oxidized system (Table 2).

DISCUSSION

We produced ternary membranes comprised of long-chain low-T_{melt} lipids, short chain high-T_{melt} lipids, and cholesterol. Given that low-T_{melt} lipids partition preferentially into the Ld phase (and high-T_{melt} lipids into the Lo phase), that single-component membranes made of the low-T_{melt} lipid are thicker than those made of the high-T_{melt} lipid, and that estimates imply that Ld phases should be thicker than Lo phases for some of the membranes (even when uncertainties are accounted for), we expected to find at least one case of a thicker Ld than Lo phase. We find none (Table 2), except when vesicles are intentionally photo-oxidized.

The reasons that thickness differences between Lo and Ld phases in ternary systems do not simply reflect thickness differences of single-component membranes arise from the fact that the Lo and Ld phases contain mixtures of the low-T_{melt} lipid, the high-T_{melt} lipid, and cholesterol.[13] Cholesterol thickens membranes. As the cholesterol fraction in a membrane increases, the Lo phase could become thicker than the Ld phase for two reasons. First, in PC-lipid membranes, the Lo phase contains higher fractions of cholesterol than the Ld phase does.[13, 41–44] Second, the Lo phase contains higher fractions of saturated lipids, and cholesterol has been reported to preferentially thicken the hydrophobic regions of single-component membranes comprised of saturated lipids more than it thickens those comprised of unsaturated lipids.[17, 48] Cholesterol likely increases the thickness of the lipid headgroup regions within membranes as well,[49] perhaps differentially. However, the reasoning above is not necessarily general. A counterexample, in which an increase in membrane cholesterol fraction correlates with a decrease in the thickness difference between the Lo and Ld phases, has been reported for membranes of 18:1-PC/16:0-PC/cholesterol and 18:1-PC/18:0-PC/cholesterol.[50]

In theory, preferential thickening of the Lo phase by cholesterol could be overcome by introducing shorter high-T_{melt} lipids or longer low-T_{melt} lipids into bilayers. However, we find that this drives the liquid-liquid coexistence region to temperatures below 25 °C (Figure 2b) or eliminates it altogether (Figure 2c). For systems that exhibit liquid-liquid phase

separation, there is no monotonic relationship between the highest T_{mix} and any of several physical parameters of the lipid components, such as the difference in thicknesses or T_{melt} values of single-component bilayers (Figure 3). This lack of a clear correlation implies that the properties of lipid mixtures depend on nuances of membrane structure that are not captured by the properties of single-component bilayers.

Taken broadly, our work shows that it is challenging to translate physical data for single-component membranes or from estimated thickness differences between Lo and Ld phases into quantitative predictions of the highest temperature at which Lo and Ld phases appear in ternary membranes. The task of predicting the highest T_{mix} is more tractable in the case that only one of the three components of the ternary membrane is varied. For example, in membranes in which a saturated lipid is mixed with 4Me-16:0-PC and cholesterol, the highest T_{mix} increases monotonically as the chain length of the saturated lipid increases. In this system, the highest T_{mix} reaches 11, 35, and 47 ± 1 °C for saturated lipids of 12:0-PC, 13:0-PC, and 16:0-PC,[41] respectively. This trend is reversed in membranes in which an unsaturated lipid is mixed with 16:0-PC and cholesterol. In this case, the highest T_{mix} increases monotonically as the chain length of the unsaturated lipid *decreases* such that the highest T_{mix} = 25, 39, and 40 ± 1 for unsaturated lipids of 22:1-PC, 20:1-PC, and 18:1-PC,[40] respectively. The reversal of the trend illustrates why predicting the highest T_{mix} for an arbitrary ternary membrane is difficult.

To date, quantitative measurements of the thickness difference between coexisting Lo and Ld phases have been reported for only a few systems.[19–31, 50] Those published data, combined with our thickness difference measurements in Table S7 provide evidence about the alignment of bilayers on solid supports. In a supported bilayer, if all phospholipid headgroups that face the substrate lie in the same plane, then any thickness mismatch is accommodated entirely in the monolayer furthest from the surface. Evidence in support of this scenario is found in some reported thickness differences between Lo and Ld phases in 40/40/20 18:1-PC/16:0-PC/cholesterol supported lipid bilayers. Measurements by AFM, which are sensitive to the difference in height between the top leaflets of each phase, give values of 1.2 ± 0.1 (from our data in Table S7), 1.2 ± 0.2, and 0.65 ± 0.02 nm.[22, 51] Our value agrees well with the results from reference 22. These AFM values are the roughly the same or larger than thickness differences between Lo and Ld phases reported by x-ray diffraction. Specifically, x-ray measurements give the thickness difference as 0.56 ± 0.2 nm (using the same ratio of lipids and reporting phosphate-to-phosphate differences)[23] or as 0.75 ± 0.3 nm (using a similar ratio of 36/41/23 18:1-PC/16:0-PC/cholesterol).[50]

On the other hand, Nielsen and Simonsen make the opposite argument[30] based on their reported thickness difference in a supported bilayer measured by ellipsometry. This technique, like X-ray diffraction, is sensitive to the total thickness difference. Their value of 1.69 nm is significantly larger than step heights reported by AFM, from which they conclude that thickness differences in supported bilayers are distributed on both faces of the membrane.

Our results, along with the data in Tables S2 through S6 in the Supporting Information, provide a broad context within which to assess supported membranes and AFM

measurements of membrane thickness. AFM is noted for its sub-Ångstrom-level height resolution, yet sample-to-sample variation in measured membrane thickness is at least one order of magnitude greater than this resolution. Moreover, different scanning methods yield different values. Previous authors have advocated the use of low-force, contact-mode methods, citing that tapping mode methods yield wide variation and/or drifts in thickness measurements.[29] Consideration of whether the AFM tip penetrates the membrane and of whether compressibilities of the two membrane phases differ significantly may also be important in some systems.[29, 52–54] Spurious height differences between phases can result from known AFM artifacts such as edge overshoot, which results from hysteresis in the z-piezoelectric ceramic, and from overly limited data as in a single line profile.[55] The AFM field has yet to converge upon a single, best method that yields a measurement of membrane thickness or of thickness mismatch that is consistently repeatable between different research groups, and details such as scanning forces are not always reported. This situation underscores the utility of interrogating the same membrane region by multiple techniques, such as fluorescence microscopy and AFM. Complementary methods of assessing membrane thicknesses include X-ray and neutron diffraction,[9–10, 23, 48, 56] cryo-electron microscopy,[57] and imaging ellipsometry.[30] A strong advantage of the experimental design of our AFM study is that it focuses on the sign of the thickness mismatch rather than the magnitude, such that the sign should be replicable by other AFM methods.

Table 2 reports a direct measurement of a thicker Ld phase, with the major caveat that the phenomenon occurs for a single lipid ratio and requires photo-oxidation, which perturbs the membrane composition. A less important caveat is that the origin and significance of the small-scale structure in Figure 4e is unclear; it may not exist in a corresponding membrane of a free-floating vesicle. For instance, submicron inhomogeneity may arise due to an offset between the temperature of the AFM and the temperature at which vesicles are ruptured, or due to a shift in miscibility transition temperature between a vesicle and a supported bilayer. Indeed, shifts in T_{mix} can result from membrane adhesion to surfaces.[58–61] As a result of such temperature shifts, the membrane may approach a critical point,[37, 42, 62] or new solid or liquid domains may nucleate but be hydrodynamically hindered from coarsening.[63–65] Temperature shifts that result in three-phase (Lo-Ld-gel) membranes provide a particularly compelling explanation of the appearance of noncircular, small domains in supported membranes made from ruptured GUVs.[42, 66]

More generally, our report of a thicker Ld than Lo phase in a photo-oxidized membrane is important because it suggests that future searches for thicker Ld phases in unoxidized membranes will eventually yield positive results. Review of the data amassed in Table 1 and Figure 3 suggests tactics to be employed in those future searches. A lack of temperature control in our AFM setup required room-temperature phase separation in membranes. Methods that assess membrane thickness below room temperature could be applied to 20:1-PC/14:0-PC/cholesterol, which is a promising system both because of the large difference in lipid tail lengths and because of implications by Lin and London that a similar system (20:1-PC/16:0-PC/14:0-PC/cholesterol) features thicker Ld than Lo phases.[35] Another tactic would be to employ chemical synthesis to produce low-T_{melt} lipids with longer methylated chains than 4Me-16:0-PC. Any tactic that involves replacing the low-T_{melt} lipid with a

polyunsaturated lipid (e.g. 22:6-PC) should be undertaken with caution because acyl chains of polyunsaturated lipids are readily photo-oxidized and because those chains are more likely than chains of singly unsaturated lipids to fold back on themselves such that their methyl carbons lie near lipid head groups, negating the expected thickening from adding carbons to the tail.[67]

CONCLUSION

We combined fluorescence microscopy and room temperature AFM to measure transition temperatures and the Lo-Ld thickness mismatch in model membranes. We used non-canonical ternary lipid mixtures for which the single-component membrane of the low-T_{melt} lipid is thicker than a single-component membrane of the high-T_{melt} lipid. We found that not one of the systems in Table 2 produced thicker Ld than Lo phases under standard experimental conditions (i.e. without photo-oxidation of the membrane). Moreover, we found no simple monotonic relationship between the highest possible miscibility transition temperature in these ternary membranes and either the estimated thickness difference between Lo and Ld phases or the relative properties of single-component membranes comprised of the low-T_{melt} and high-T_{melt} lipids. It is a common[68–69] and even textbook assertion[70–71] that rafts within cell membranes contain lipids with more ordered acyl chains and that they are thicker than the surrounding cell membrane. Even when we employed the noncanonical lipid mixtures in Table 1, we found no physical reason to challenge this assertion. Future direct searches for thicker Ld regions may find it productive to employ low-temperature methods or to incorporate lipids with longer methylated chains in the membranes.

MATERIALS AND METHODS

Lipids

All phosphocholine (PC) lipids (Avanti Polar Lipids, Alabaster, AL), Texas Red dihexadecanoyl-PE (DHPE; Life Technologies, Grand Island, NY), and cholesterol (chol; Sigma, St. Louis, MO) were purchased and used without further purification. The PC-lipids and their single-component membrane T_{melt} values are as follows: dilauroyl-PC (12:0-PC, −2 °C), ditridecanoyl-PC (13:0-PC, 14 °C), dimyristoyl-PC (14:0-PC, 24°C), dipalmitoyl-PC (16:0-PC, 41 °C), diheptadecanoyl-PC (17:0-PC, 50 °C), distearoyl-PC (18:0-PC, 55 °C), dioleoyl-PC (18:1-PC, −17 °C), dieicosenoyl-PC (20:1-PC, −4 °C), dierucoyl-PC (22:1-PC, 13 °C), dinervonoyl-PC (24:1-PC, 27 °C), and diphytanoyl-PC (4Me-16:0-PC, < −120 °C).[72–74] Structures of the lipids are given in Figure S1.

Estimates of thickness differences between Lo and Ld membrane phases

For the ternary systems in Table 1, a single-component liquid membrane comprised of the disordered lipid alone is *thicker* than a single-component liquid membrane comprised of the ordered lipid alone. Because published values of these thicknesses were collected at different temperatures (listed in Fig. S1) rather than at a single temperature and because the systems in Table 1 contain cholesterol, we also produced rough estimates of thickness differences between Lo and Ld phases of the ternary systems near room temperature.

Given that tie lines are not known for the systems in Table 1 and that thicknesses have been measured for few membranes containing PC-lipids and cholesterol, our estimates necessarily rest upon broad assumptions. The first assumption is that the acyl chains of the PC-lipids in the Lo phase are sufficiently extended that the thickness of the Lo phase is equivalent to the thickness of a gel phase of a pure PC-lipid membrane. X-ray measurements at 25 °C for bilayers of pure, gel phase 16:0-PC, 18:0-PC, 20:0-PC, 22:0-PC and 24:0-PC yield phosphate-to-phosphate distances of 42.8 Å, 47.0 Å, 50.6 Å, 53.9Å, and 57.9 Å, respectively.[18] These values are well fit by a line. We extrapolate this line in order to estimate thicknesses of bilayers of 12:0-PC, 13:0-PC, 14:0-PC, and 17:0-PC to be 35.3 Å, 37.1 Å, 39 Å, and 44.5 Å, respectively. Illustrating the paucity of the available data and the roughness of our estimate, phosphate-to-phosphate distances for membranes containing binary mixtures of saturated PC-lipids and cholesterol have been published for only 70/30 14:0-PC/cholesterol to our knowledge, and the distance is a few Ångstroms larger than for gel-phase 14:0-PC.[17]

Our second assumption is that thicknesses of Ld phases containing 20:1-PC and 24:1-PC can be found by extrapolating published values of phosphate-to-phosphate distances for bilayers of 18:1-PC and 22:1-PC with 30 mol% cholesterol at 30 °C.[17] These values are 39.9 Å and 47.1 Å and yield thicknesses of 43.5 Å and 50.7 Å for Ld phases containing 20:1-PC and 24:1-PC, respectively. Our third assumption is that the thickness of the Ld phase in bilayers containing 4Me-16:0-PC is equivalent to the phosphate-to-phosphate distance of a pure bilayer of 4Me-16:0-PC at 30 °C obtained by joint analysis of neutron and X-ray scattering data, which is 35.2 Å.[10] Uncertainties in these values are on the order of an Ångstrom given that two different methods of fitting the data for pure 4Me-16:0-PC bilayers results in phosphate-to-phosphate distances that differ by ~1 Å. Further refinements of these estimates would result in changes that are smaller than the uncertainties. For example, using thermal contractivities of membranes to correct for the difference between experimental temperatures of 25 °C for high-T_{melt} lipids and 30 °C for low-T_{melt} lipids would result in a shift of ~0.3 Å. Converting phosphate-to-phosphate distances to Luzzati thicknesses for all membranes would result in offsets in the thicknesses of both the Lo and Ld phases, and no substantial change in the thickness difference.

Overview

To avoid the problem that sonicated vesicles, which are commonly used in AFM studies to produce supported lipid bilayers, do not always contain the same lipid and sterol composition as the large vesicles from which they are made,[75] we interrogated GUVs. Miscibility phase behavior was determined by fluorescence microscopy of intact, free-floating giant unilamellar vesicles. Thicknesses of the two liquid phases were determined by AFM of supported lipid bilayers made by rupturing GUVs of the same composition.

Preparation of GUVs

Taut GUVs were produced by electroformation[11, 76] at 60 °C for 1 hr. with the application of 1.5 V at 10 Hz. Vesicles to be assessed by AFM were made in 200 mM sucrose; the freshly-made vesicle solution was cooled to room temperature and diluted in 3 mL of 200 mM sucrose. Vesicles to be assessed by fluorescence microscopy alone were made in 18

MΩ-cm water and further diluted before viewing. Electroformation in sucrose does not significantly shift T_{mix} for vesicles containing zwitterionic lipids (as opposed to those containing lipids with a net charge).[77] Vesicles for fluorescence microscopy were labeled with 0.8 mol% Texas Red DHPE[78] and used within 4 hours of electroformation. To prevent unintentional photooxidation of lipids during the preparation and handling of samples containing unsaturated lipids (namely, 20:1-PC and 22:1-PC), lipid stock solutions and electroformation plates were shielded from light by a protective covering of aluminum foil. Electroformation chambers containing these lipids were assembled in a darkened room in which all lamps and lights were turned off; dim illumination came from indirect, diffuse natural light through a shaded window.

Photon power and flux of fluorescence microscopes

Photon power was measured with a calibrated silicon photodiode (OSI-Optoelectronics, Horten, Norway) with a Keithley (Cleveland, OH) 2400 sourcemeter and an Ocean Optics (Dunedin, FL) USB2000+spectrometer. To convert power to photon flux for the broadband light sources of the fluorescence microscopes, we divided the total power by the weighted average photon energy. We obtained this average photon energy in Joules/photon by integrating the emission spectrum weighted by the photon energy at each wavelength. Two fluorescence microscopes were used in this study. The microscope used to measure T_{mix} delivered 1.65×10^{-3} W of power to the sample under the conditions of our measurement, resulting in a flux of 4.70×10^{15} photons/s. The microscope coupled to the AFM delivered 2.70×10^{-3} W of photon power to the sample under the conditions of our measurement, with a flux of 7.70×10^{15} photons/s.

Determination of T_{mix} in GUVs

Vesicles were imaged by fluorescence microscopy and T_{mix} values were determined as described in detail previously.[37, 40] Briefly, the vesicle solution was placed between two coverslips, sealed with vacuum grease, and thermally coupled to a temperature-controlled stage on a fluorescence microscope. As temperature decreased, the percentage of vesicles exhibiting micron-scale liquid-liquid phase separation was recorded, and the resulting data were fit with a sigmoidal curve to determine T_{mix}, the temperature at which 50% of vesicles phase separated. Variation in T_{mix} arises from small vesicle-to-vesicle compositional differences.[11] Gel domains were visually identified by their lack of coalescence and rigid, noncircular shapes; liquid domains are circular and coalesce.[65, 79]

Precautions were taken to limit light exposure of vesicles during measurements of T_{mix}. This is important because light increases T_{mix} in vesicles containing fluorescence labels and unsaturated lipids, such that membrane domains nucleate[36, 38–39, 47, 79]. Vesicle samples containing either 20:1-PC or 22:1-PC lipids were treated as follows. A single aliquot was taken from the sample and placed between glass coverslips sealed with vacuum grease. This coverslip assembly was placed on a temperature controlled microscope stage, with illumination blocked by a shutter. After the temperature equilibrated, the shutter was opened, and vesicles were observed through a 40× objective under the lowest light conditions that produced a clear image. Specifically, light reaching the sample through the fluorescence microscope was attenuated simultaneously by 4× and 16× neutral density

filters. Photon power and flux of this attenuated beam are listed in the photon power section above. Cumulative light exposure was minimized by imaging an aliquot at only one temperature, and then replacing it with a new one. In other words, after images were collected at one temperature, the coverslip assembly was discarded, and the temperature was changed to a new value. A new coverslip assembly containing a new aliquot of the same stock vesicle sample was used to collect images at the new temperature. This procedure continued until images were collected at all temperatures. All images and aliquots in which domains were observed to nucleate in response to light were discarded.

Rupture of GUVs into spatially separated supported lipid bilayers

The top layers of a mica disk (Highest Grade V1, Ted Pella, Redding, CA) were cleaved with Scotch tape (3M, St. Paul, MN) to reveal a clean, smooth surface. Then 500 μL of 200 mM glucose/5mM $CaCl_2$ was pipetted onto the mica, followed by 50 μL of GUV-rich sucrose solution. After 15 min., the bilayer was rinsed with 1 mL aliquots of water 20 times, taking care that the surface was never exposed to air. This process resulted in a mica surface densely covered with individual supported lipid bilayers separated by areas of bare mica (Figure 1b). This surface remained submerged under water for the remainder of the experiment.

Conservation of area fraction upon GUV rupture

In Figure 1b, the total surface area of the free-floating vesicle was the same ($2.57 \pm 0.40 \times 10^3$ μm^2) within uncertainty as the supported lipid bilayer that it became ($2.50 \pm 0.08 \times 10^3$ μm^2). The average area fraction of the Ld phase was the same before (75 ± 4%) and after rupture (77 ± 2%). Reported uncertainties are the standard deviations of area fractions determined using the inner and the outer edges of the vesicle, specifically the inner and outer the edges determined after Canny-Deriche filtering of the image for edge detection (setting parameter $\alpha = 1.00$ in ImageJ[80]). The observation of equivalent area fractions in free-floating vesicles and supported lipid bilayers is consistent with an absence of a significant shift in miscibility tie-line endpoints upon rupture.

Measuring Lo:Ld area fractions

To determine Lo:Ld area ratios, free-floating, fluorescently labeled GUVs were imaged with light from a mercury arc light source (USH-102DH, Ushio, Tokyo, Japan) that was filtered through a Texas Red HYQ filter, which was housed within a Nikon YFL microscope equipped with a 40×, 0.60 N.A. objective (Nikon, Melville, NY). The GUVs were ruptured onto a mica disk to form supported lipid bilayers as described above, and the area ratio was measured again by fluorescence microscopy. Fluorescence images were captured on a Coolsnap HQ charge-coupled device camera (Photometrics, Tucson, AZ).

AFM decoupled from fluorescence microscopy

GUVs were ruptured onto a mica disk to form supported lipid bilayers. The disk was adhered with Vaseline (Unilever, Englewood Cliffs, NJ) to the bottom of a perfusion cell (Bruker, Santa Barbara, CA). Images were acquired on a Dimension Icon Atomic Force Microscope (Bruker, Santa Barbara, CA) in quantitative nanomechanical mapping mode

using SCANASYST-AIR cantilevers (k = 0.4 N/m, Bruker). We determined the thick:thin area ratio of an individual supported lipid bilayer by imaging its entire surface. We compared the Lo:Ld area ratio to the thick:thin area ratio in order to associate the phases measured by AFM with the phases measured by fluorescence.

AFM coupled with fluorescence microscopy

Fluorescently labeled vesicles of 20/55/25 mol% 22:1-PC/16:0-PC/chol were introduced to a solution of 200 mM glucose/5mM $CaCl_2$ above a mica substrate and were intentionally exposed to light over the course of 5 min. as they settled to the surface. The light was produced by a mercury arc lamp (USH-102DH, Ushio, Tokyo, Japan) and was filtered through a Texas Red HYQ filter block (Nikon). After the vesicles deposited and ruptured on the surface, they were imaged on a Nikon YFL microscope illuminated by the same filtered light source focused on the sample through a CFI Plan Fluor 60× objective (Nikon).

Our procedure of intentional light exposure was necessary; vesicles that remained outside of the light path as they settled to the surface exhibited no large scale phase separation. Likewise, no phase separation was observed in supported lipid bilayers formed from vesicles that were deposited and ruptured on mica substrates in a darkened room in which all lamps and lights were turned off and in which illumination came only from dim, indirect natural light through a shaded window. The requirement of intense illumination to achieve large scale phase separation within GUVs of 22:1-PC/16:0-PC/chol is surprising because free floating vesicles of the same composition required no previous light exposure during determination of T_{mix}.

Observation of large scale phase separation after intentional exposure to light is consistent with previous reports of photooxidation of unsaturated lipids.[36, 38–39, 47] In our system of GUVs of 22:1-PC/16:0-PC/chol, when the concentration of Texas Red DHPE was decreased from 0.8 mol% to 0.2 mol%, less than 10% of vesicles exposed to light exhibited large scale phase separation, even after several minutes of exposure.

Supported bilayers were imaged with an MFP-3D-BIO Atomic Force Microscope (Asylum Research) seated on a Nikon Eclipse Ti microscope.[81] Fluorescence images were captured on a Spot FX1520 CCD Camera (Spot Imaging Solutions, Sterling Heights, MI). Scans were performed in contact mode using DNP-10 tips (0.12 N/m, Bruker) at a constant scanning force from 0.2 – 0.4 nN, such that experiments here and by other researchers[29] were conducted under the same conditions.

AFM image processing

AFM images were flattened in Gwyddion as described in the Supporting Information.[82] Height histograms were exported to MATLAB (MathWorks, Natick, MA) and fit with two Gaussian peaks corresponding to the thick and thin phases using the program ipf.m[83] as described in methods in the Supporting Information. Reported membrane thicknesses are differences between the centers of these peaks and are summarized in Tables S2–S6.

Supplementary Material

Refer to Web version on PubMed Central for supplementary material.

Acknowledgments

This research was supported by the National Science Foundation MCB07444852 and MCB1402059. J.V.B. was supported by NIH Training in Molecular Biophysics T32 GM008268. P.A.C. acknowledges support from NSF DMR-1306079. P.A.C. and the laboratory of David Ginger thank AFOSR for supporting instrumentation of an AFM coupled to a fluorescence light source. J.P.L. was supported by National Science Foundation Graduate Research Fellowship DGE0718124. D.G.C. and R.N.F. were supported by NIH grant EB-002027 to the National ECSA and Surface Analysis Center for Biomedical Problems (NESAC/BIO). S.L.K. acknowledges support from the Miller Institute for Basic Research in Science, University of California Berkeley. We thank Scott Rayermann for comments on our manuscript. We thank an anonymous reviewer for guidance in estimating membrane thicknesses.

ABBREVIATIONS

T_{melt}	melting temperature
T_{mix}	miscibility transition temperature
GUV	giant unilamellar vesicle
Ld	liquid disordered phase
Lo	liquid ordered phas
AFM	atomic force microscopy

REFERENCES

1. Andersen OS, Koeppe RE II. Bilayer Thickness and Membrane Protein Function: An Energetic Perspective. Annu. Rev. Biophys. Biomol. Struct. 2007; 36:107–130. [PubMed: 17263662]
2. Phillips R, Ursell T, Wiggins P, Sens P. Emerging Roles for Lipids in Shaping Membrane-Protein Function. Nature. 2009; 459:379–385. [PubMed: 19458714]
3. Heimburg, T. Thermal Biophysics of Membranes. Weinheim: Wiley-VCH; 2007.
4. Simons K, Ikonen E. Functional Rafts in Cell Membranes. Nature. 1997; 387:569–572. [PubMed: 9177342]
5. Simons K, Gerl MJ. Revitalizing Membrane Rafts: New Tools and Insights. Nat. Rev. Mol. Cell. Bio. 2010; 11:688–699. [PubMed: 20861879]
6. Lewis BA, Engelman DM. Lipid Bilayer Thickness Varies Linearly with Acyl Chain Length in Fluid Phosphatidylcholine Vesicles. J. Mol. Biol. 1983; 166:211–217. [PubMed: 6854644]
7. Petrache HI, Dodd SW, Brown MF. Area Per Lipid and Acyl Length Distributions in Fluid Phosphatidylcholines Determined by ^{2}H NMR Spectroscopy. Biophys. J. 2000; 79:3172–3192. [PubMed: 11106622]
8. Sperotto MM, Mouritsen OG. Dependence of Lipid Membrane Phase Transition Temperature on the Mismatch of Protein and Lipid Hydrophobic Thickness. Eur. Biophys. J. 1988; 16:1–10.
9. Kučerka N, Gallová J, Uhríková D, Balgavy P, Bulacu M, Marrink S-J, Katsaras J. Areas of Monounsaturated Diacylphosphatidylcholines. Biophys. J. 2009; 97:1926–1932. [PubMed: 19804723]
10. Kučerka N, Nieh M-P, Katsaras J. Fluid Phase Lipid Areas and Bilayer Thicknesses of Commonly Used Phosphatidylcholines as a Function of Temperature. Biochim. Biophys. Acta. 2011; 1808:2761–2771. [PubMed: 21819968]
11. Veatch SL, Keller SL. Seeing Spots: Complex Phase Behavior in Simple Membranes. Biochim. Biophys. Acta. 2005; 1746:172–185. [PubMed: 16043244]

12. Ipsen JH, Karlström G, Mouritsen OG, Wennerström H, Zuckermann MJ. Phase Equilibria in the Phosphatidylcholine-Cholesterol System. Biochim. Biophys. Acta. 1987; 905:162–172. [PubMed: 3676307]
13. Veatch SL, Polozov IV, Gawrisch K, Keller SL. Liquid Domains in Vesicles Investigated by NMR and Fluorescence Microscopy. Biophys. J. 2004; 86:2910–2922. [PubMed: 15111407]
14. Baumgart T, Hunt G, Farkas ER, Webb WW, Feigenson GW. Fluorescence Probe Partitioning between Lo/Ld Phases in Lipid Membranes. BBA - Biomembranes. 2007; 1768:2182–2194. [PubMed: 17588529]
15. Sengupta P, Hammond A, Holowka D, Baird B. Structural Determinants for Partitioning of Lipids and Proteins between Coexisting Fluid Phases in Giant Plasma Membrane Vesicles. Biochim. Biophys. Acta. 2008; 1778:20–32. [PubMed: 17936718]
16. Stillwell, W. An Introduction to Biological Membranes: From Bilayers to Rafts. London: Elsevier; 2013.
17. Pan J, Tristram-Nagle S, Nagle JF. Effect of Cholesterol on Structural and Mechanical Properties of Membranes Depends on Lipid Chain Saturation. Phys. Rev. E. 2009; 80:021931, 1–12.
18. Sun W-J, Tristram-Nagle S, Suter RM, Nagle JF. Structure of Gel Phase Saturated Lecithin Bilayers: Temperature and Chain Length Dependence. Biophys. J. 1996; 71:885–891. [PubMed: 8842227]
19. Rinia HA, Snel MME, van der Eerden JPJM, de Kruijff B. Visualizing Detergent Resistant Domains in Model Membranes with Atomic Force Microscopy. FEBS Lett. 2001; 501:92–96. [PubMed: 11457463]
20. Berquand A, Mingeot-Leclercq MP, Dufrene YF. Real-Time Imaging of Drug-Membrane Interactions by Atomic Force Microscopy. Biochim. Biophys. Acta. 2004; 1664:198–205. [PubMed: 15328052]
21. Giocondi M-C, Le Grimellec C. Temperature Dependence of the Surface Topology in Dimyristoylphosphatidylcholine/Distearoylphosphatidylcholine Multibilayers. Biophys. J. 2004; 86:2218–2230. [PubMed: 15041661]
22. Jensen MH, Morris EJ, Simonsen AC. Domain Shapes, Coarsening, and Random Patterns in Ternary Membranes. Langmuir. 2007; 23:8135–8141. [PubMed: 17590026]
23. Chen L, Yu Z, Quinn PJ. The Partition of Cholesterol between Ordered and Fluid Bilayers of Phosphatidylcholine: A Synchrotron X-Ray Diffraction Study. Biochim. Biophys. Acta. 2007; 1768:2873–2881. [PubMed: 17900525]
24. Garcia-Saéz AJ, Chiantia S, Schwille P. Effect of Line Tension on the Lateral Organization of Lipid Membranes. J. Biol. Chem. 2007; 282:33537–33544. [PubMed: 17848582]
25. Mills TT, Tristram-Nagle S, Heberle FA, Morales NF, Zhao J, Wu J, Toombes GES, Nagle JF, Feigenson GW. Liquid-Liquid Domains in Bilayers Detected by Wide Angle X-Ray Scattering. Biophys. J. 2008; 95:682–690. [PubMed: 18390623]
26. Weise K, Triola G, Brunsveld L, Waldmann H, Winter R. Influence of the Lipidation Motif on the Partitioning and Association of N-Ras in Model Membrane Subdomains. J. Am. Chem. Soc. 2009; 131:1557–1564. [PubMed: 19133719]
27. Goksu EI, Longo ML. Ternary Lipid Bilayers Containing Cholesterol in a High Curvature Silica Xerogel Environment. Langmuir. 2010; 26:8614–8624. [PubMed: 20143868]
28. Marques JT, de Almeida RFM, Viana AS. Biomimetic Membrane Rafts Stably Supported in Unmodified Gold. Soft Matter. 2012; 8:2007–2016.
29. Connell SD, Heath G, Olmsted PD, Kisil A. Critical Point Fluctuations in Supported Lipid Membranes. Faraday Discuss. 2013; 161:91–111. [PubMed: 23805740]
30. Nielsen MMB, Simonsen AC. Imaging Ellipsometry of Spin-Coated Membranes: Mapping of Multilamellar Films, Hydrated Membranes, and Fluid Domains. Langmuir. 2013; 29:1525–1532. [PubMed: 23281595]
31. Heberle FA, Petruzielo RS, Pan J, Drazba P, Kučerka N, Standaert RF, Feigenson GW, Katsaras J. Bilayer Thickness Mismatch Controls Domain Size in Model Membranes. J. Am. Chem. Soc. 2013; 135:6853–6859. [PubMed: 23391155]

32. Kuzmin PI, Akimov SA, Chizmadzhev YA, Zimmerberg J, Cohen FS. Line Tension and Interaction Energies of Membrane Rafts Calculated from Lipid Splay and Tilt. Biophys. J. 2005; 88:1120–1133. [PubMed: 15542550]
33. Wallace EJ, Hooper NM, Olmsted PD. Effect of Hydrophobic Mismatch on Phase Behavior of Lipid Membranes. Biophys. J. 2006; 90:4104–4118. [PubMed: 16533859]
34. Williamson JJ, Olmsted PD. Registered and Antiregistered Phase Separation of Mixed Amphiphilic Bilayers. Biophys. J. 2015; 108:1963–1976. [PubMed: 25902436]
35. Lin Q, London E. Altering Hydrophobic Sequence Length Shows That Hydrophobic Mismatch Controls Affinity for Ordered Lipid Domains (Rafts) in the Multitransmembrane Strand Protein Perfringolysin O*. J. Biol. Chem. 2013; 288:1340–1352. [PubMed: 23150664]
36. Ayuyan AG, Cohen FS. Lipid Peroxides Promote Large Rafts: Effects of Excitation of Probes in Fluorescence Microscopy and Electrochemical Reactions During Vesicle Formation. Biophys. J. 2006; 91:2172–2183. [PubMed: 16815906]
37. Honerkamp-Smith AR, Cicuta P, Collins MD, Veatch SL, den Nijs M, Schick M, Keller SL. Line Tensions, Correlation Lengths, and Critical Exponents in Lipid Membranes near Critical Points. Biophys. J. 2008; 95:236–246. [PubMed: 18424504]
38. Roux A, Cuvelier D, Nassoy P, Prost J, Bassereau P, Goud B. Role of Curvature and Phase Transition in Lipid Sorting and Fission of Membrane Tubules. EMBO J. 2005; 24:1537–1545. [PubMed: 15791208]
39. Morales-Penningston NF, Wu J, Farkas ER, Goh SL, Konyakhina TM, Zheng JY, Webb WW, Feigenson GW. Guv Preparation and Imaging: Minimizing Artifacts. Biochim. Biophys. Acta. 2010; 1798:1324–1332. [PubMed: 20302841]
40. Veatch SL, Keller SL. Separation of Liquid Phases in Giant Vesicles of Ternary Mixtures of Phospholipids and Cholesterol. Biophys. J. 2003; 85:3074–3083. [PubMed: 14581208]
41. Veatch SL, Gawrisch K, Keller SL. Closed-Loop Miscibility Gap and Quantitative Tie-Lines in Ternary Membranes Containing Diphytanoyl Pc. Biophys. J. 2006; 90:4428–4436. [PubMed: 16565062]
42. Veatch SL, Soubias O, Keller SL, Gawrisch K. Critical Fluctuations in Domain-Forming Lipid Mixtures. Proc. Natl. Acad. Sci. USA. 2007; 104:17650–17655. [PubMed: 17962417]
43. Davis JH, Clair JJ, Juhasz J. Phase Equilibria in Dopc/Dppc-D62/Cholesterol Mixtures. Biophys. J. 2009; 96:521–539. [PubMed: 19167302]
44. Heberle FA, Wu J, Goh SL, Petruzielo RS, Feigenson GW. Comparison of Three Ternary Lipid Bilayer Mixtures: Fret and Esr Reveal Nanodomains. Biophys. J. 2010; 99:3309–3318. [PubMed: 21081079]
45. Ionova IV, Livshits VA, Marsh D. Phase Diagram of Ternary Cholesterol / Palmitoylsphingomyelin / Palmitoyloleoyl-Phosphatidylcholine Mixtures: Spin-Label Epr Study of Lipid-Raft Formation. Biophys. J. 2012; 102:1856–1865. [PubMed: 22768941]
46. Bezlyepkina N, Gracia RS, Shchelokovskyy P, Lipowsky R, Dimova R. Phase Diagram and Tie-Line Determination for the Ternary Mixture Dopc/Esm/Cholesterol. Biophys. J. 2013; 104:1456–1464. [PubMed: 23561522]
47. Veatch SL, Leung SSW, Hancock REW, Thewalt JL. Fluorescent Probes Alter Miscibility Phase Boundaries in Ternary Vesicles. J. Phys. Chem. B. 2007; 111:502–504. [PubMed: 17228905]
48. Hung W-C, Lee M-T, Chen F-Y, Huang HW. The Condensing Effect of Cholesterol in Lipid Bilayers. Biophys. J. 2007; 92:3960–3967. [PubMed: 17369407]
49. Pan J, Cheng X, Heberle FA, Mostofian B, Kučerka N, Drazba P, Katsaras J. Interactions between Ether Phospholipids and Cholesterol as Determined by Scattering and Molecular Dynamics Simulations. J. Phys. Chem. B. 2012; 116:14829–14838. [PubMed: 23199292]
50. Heftberger P, Kollmitzer B, Reider AA, Amenitsch H, Pabst G. In Situ Determination of Structure and Fluctuations of Coexisting Fluid Membrane Domains. Biophys. J. 2015; 108:854–862. [PubMed: 25692590]
51. Marques JT, Viana AS, De Almeida RFM. Ethanol Effects on Binary and Ternary Supported Lipid Bilayers with Gel/Fluid Domains and Lipid Rafts. Biochim. Biophys. Acta. 2011; 1808:405–414. [PubMed: 20955684]

52. Das C, Sheikh KH, Olmsted PD, Connell SD. Nanoscale Mechanical Probing of Supported Lipid Bilayers with Atomic Force Microscopy. Phys. Rev. E. 2010; 82:041920, 1–6.
53. Dufrene YF, Barger WR, Green J-BD, Lee GU. Nanometer-Scale Surface Properties of Mixed Phospholipid Monolayers and Bilayers. Langmuir. 1997; 13:4779–4784.
54. Picas L, Rico F, Scheuring S. Direct Measurement of the Mechanical Properties of Lipid Phases in Supported Bilayers. Biophys. J. 2012; 102:L01–L03. [PubMed: 22225813]
55. Eaton, P.; West, P. Atomic Force Microscopy. New York: Oxford University Press; 2010.
56. Kučerka N, Nagle JF, Sachs JN, Feller SE, Pencer J, Jackson A, Katsaras J. Lipid Bilayer Structure Determined by the Simultaneous Analysis of Neutron and X-Ray Scattering Data. Biophys. J. 2008; 95:2356–2367. [PubMed: 18502796]
57. Tahara Y, Fujiyoshi Y. A New Method to Measure Bilayer Thickness: Cryo-Electron Microscopy of Frozen Hydrated Liposomes and Image Simulation. Micron. 1994; 25:141–149. [PubMed: 8055245]
58. Kaizuka Y, Groves JT. Structure and Dynamics of Supported Intermembrane Junctions. Biophys. J. 2004; 86:905–912. [PubMed: 14747326]
59. Gordon VD, Deserno M, Andrew CMJ, Egelhaaf SU, Poon WCK. Adhesion Promotes Phase Separation in Mixed-Lipid Membranes. Eur. Phys. Lett. 2008; 84:48003, 1–5.
60. Zhao J, Wu J, Veatch SL. Adhesion Stabilizes Robust Lipid Heterogeneity in Supercritical Membranes at Physiological Temperature. Biophys. J. 2013; 104:825–834. [PubMed: 23442961]
61. Blosser MC, Honerkamp-Smith AR, Han T, Haataja M, Keller SL. Transbilayer Colocalization of Lipid Domains Explained Via Measurement of Strong Coupling Parameters. Biophys. J. 2015; 109:2317–2327. [PubMed: 26636943]
62. Honerkamp-Smith AR, Veatch SL, Keller SL. An Introduction to Critical Points for Biophysicists; Observations of Compositional Heterogeneity in Lipid Membranes. Biochim. Biophys. Acta. 2009; 1788:53–63. [PubMed: 18930706]
63. Stone HA, Ajdari A. Hydrodynamics of Particles Embedded in a Flat Surfactant Layer Overlying a Subphase of Finite Depth. J. Fluid Mech. 1998; 369:151–173.
64. Stottrup BL, Veatch SL, Keller SL. Nonequilibrium Behavior in Supported Lipid Membranes Containing Cholesterol. Biophys. J. 2004; 86:2942–2950. [PubMed: 15111410]
65. Stanich CA, Honerkamp-Smith AR, Putzel GG, Warth CS, Lamprecht AK, Mandal P, Mann E, Hua T-AD, Keller SL. Coarsening Dynamics of Domains in Lipid Membranes. Biophys. J. 2013; 105:444–454. [PubMed: 23870265]
66. Bhatia T, Husen P, Ipsen JH, Bagatolli LA, Simonsen AC. Fluid Domain Patterns in Free-Standing Membranes Captured on a Solid Support. Biochim. Biophys. Acta. 2014; 1838:2503–2510. [PubMed: 24866014]
67. Mihailescu M, Vaswani RG, Jardón-Valadez E, Castro-Román F, Freites JA, Worcester DL, Chamberlin AR, Tobias DJ, White SH. Acyl-Chain Methyl Distributions of Liquid-Ordered and Liquid-Disordered Membranes. Biophys. J. 2011; 100:1455–1462. [PubMed: 21402027]
68. Simons K, Sampaio JL. Membrane Organization and Lipid Rafts. Cold Spring Harb Perspect Biol. 2011; 3:a004697, 1–17. [PubMed: 21628426]
69. Pike LJ. The Challenge of Lipid Rafts. J. Lipid Res. 2009; 50:S323–S328. [PubMed: 18955730]
70. Lehninger, AL.; Nelson, DL.; Cox, MM. Principles of Biochemistry. Fourth. New York: W.H. Freeman; 2005.
71. Alberts, B.; Johnson, A.; Lewis, J.; Raff, M.; Roberts, K. Molecular Biology of the Cell. 4th. New York: Garland Science; 2002.
72. Lindsey H, Petersen NO, Chan SI. Physicochemical Characterization of 1,2-Diphytanoyl-Sn-Glycero-3-Phosphocholine in Model Membrane Systems. Biochim. Biophys. Acta. 1979; 555:147–167. [PubMed: 476096]
73. Silvius, JR. Lipid-Protein Interactions. New York: John Wiley & Sons; 1982. Thermotropic Phase Transitions of Pure Lipids in Model Membranes and Their Modifications by Membrane Proteins.
74. Marsh, D. Crc Handbook of Lipid Bilayers. Boca Raton, FL: CRC Press; 1990.

75. Sokolov A, Radhakrishnan A. Accessibility of Cholesterol in Endoplasmic Reticulum Membranes and Activation of Srebp-2 Switch Abruptly at a Common Cholesterol Threshold. J Biol. Chem. 2010; 285:29480–29490. [PubMed: 20573965]

76. Angelova MI, Soléau S, Méléard P, Faucon JF, Bothorel P. Preparation of Giant Vesicles by External Ac Electric Fields. Prog. Colloid Polym. Sci. 1992; 89:127–131.

77. Blosser MC, Starr JB, Turtle CW, Ashcraft J, Keller SL. Minimal Effect of Lipid Charge on Membrane Miscibility Phase Behavior in Three Ternary Systems. Biophys. J. 2013; 104:2629–2638. [PubMed: 23790371]

78. Johnson SA, Stinson BM, Go MS, Carmona LM, Reminick JI, Fang X, Baumgart T. Temperature-Dependent Phase Behavior and Protein Partitioning in Giant Plasma Membrane Vesicles. Biochim. Biophys. Acta. 2010; 1798:1427–1435. [PubMed: 20230780]

79. Blosser, MC.; Cornell, C.; Rayermann, SP.; Keller, SL. Phase Diagrams and Tie Lines in Guvs. In: Dimova, R.; Marques, C., editors. The Giant Vesicle Book. in press

80. Rasband, WS. Image J. Bethesda, MD: U.S. National Institutes of Health; p. 1997-2015.Http://Imagej.Nih.Gov/Ij

81. Cox PA, Waldow DA, Dupper TJ, Jesse S, Ginger DS. Mapping Nanoscale Variations in Photochemical Damage of Polymer/Fullerene Solar Cells with Dissipation Imaging. ACS Nano. 2013; 7:10405–10413. [PubMed: 24138326]

82. Nečas D, Klapetek P. Gwyddion: An Open-Source Software for Spm Data Analysis. Cent. Eur. J. Phys. 2012; 10:181–188.

83. O'Haver T. Ipf.M Peak Fitter. Http://Terpconnect.Umd.Edu/~Toh/Spectrum/Interactivepeakfitter.Htm.

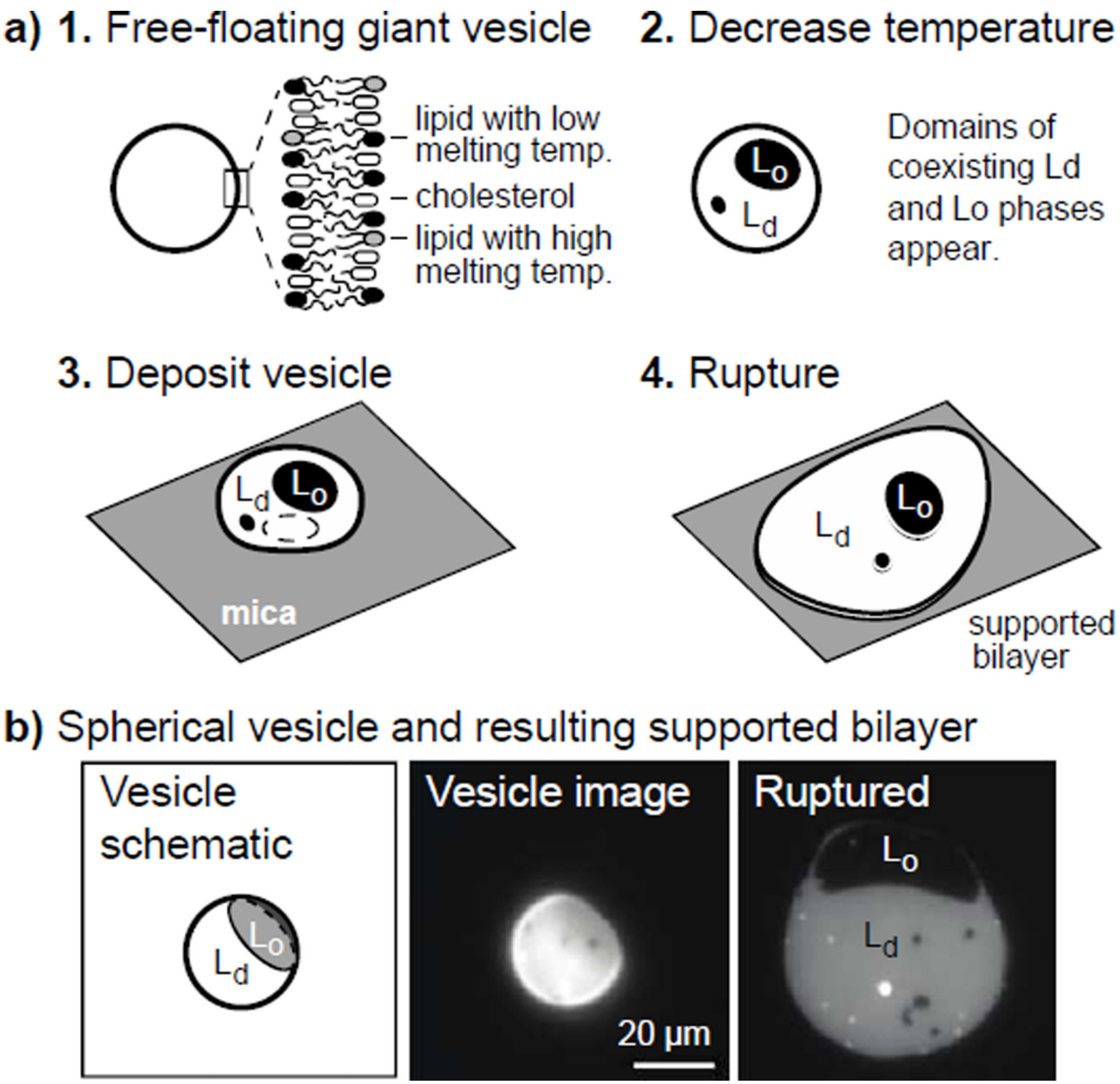

Figure 1.

(a) Schematic of procedure to rupture phase-separated giant unilamellar vesicles (GUVs) to form isolated supported lipid bilayers. (b) A phase-separated vesicle rests on a mica substrate, shown schematically in the left panel and in a fluorescence image in the center panel. The right panel shows the supported lipid bilayer that formed from the ruptured vesicle. The bilayer is comprised of 40/40/20 mol% 18:1-PC/16:0-PC/cholesterol and 0.8 mol% Texas Red DHPE.

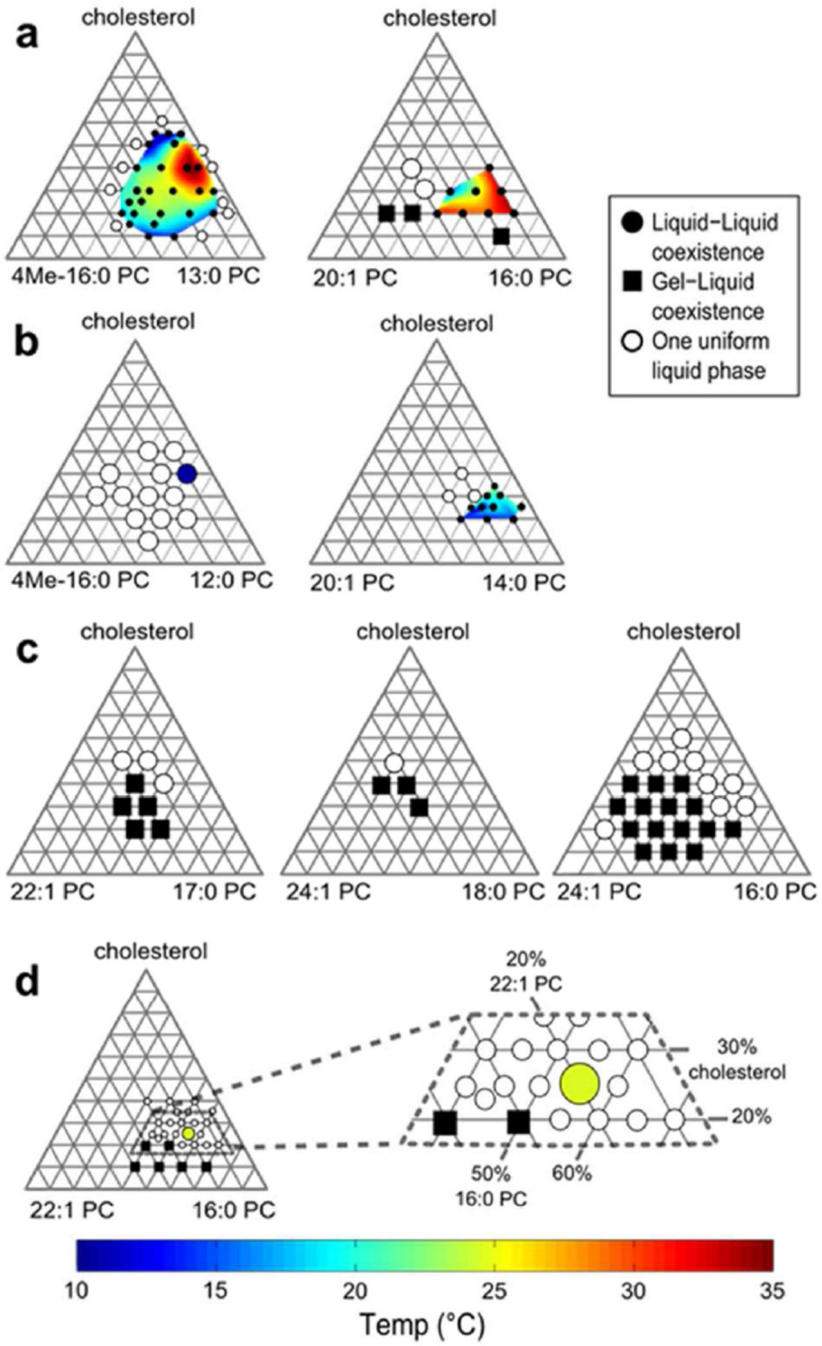

Figure 2.

Miscibility phase diagrams of giant unilamellar vesicles (GUVs) as determined by fluorescence microscopy. Points within each triangle in the figure denote ratios of the three components. The colored regions in Figure 2a,b denote the liquid-liquid coexistence regions and the corresponding T_{mix}. The single colored circles in the leftmost panels of rows b and d give the single ratio of lipids that separate into coexisting liquid phases between 10 – 50 °C in those systems. Rows differentiate membranes with ternary compositions that (a) exhibit coexisting liquid phases at or above 25 °C, (b) exhibit coexisting liquid phases only below

25 °C, (c) do not exhibit coexisting liquid phases, (d) exhibit coexisting liquid phases only after exposure to light. The two systems in row a and the system in row d were also investigated with room-temperature AFM.

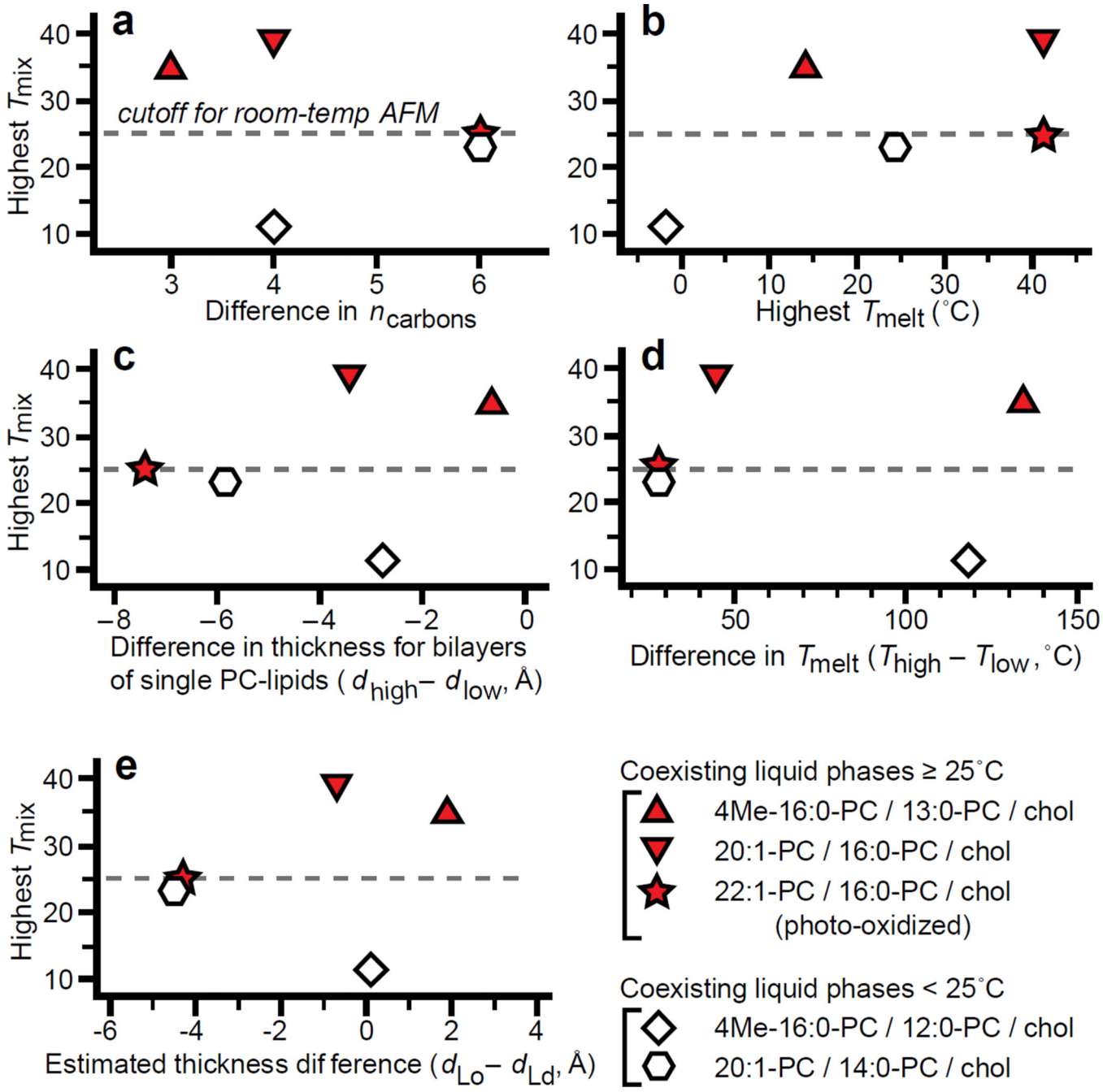

Figure 3.

Data demonstrating a lack of correlation between the highest T_{mix} of five different ternary membranes and the physical parameters of single-component membranes of the constituent PC-lipids (panels a–d) or the estimated thickness difference between the Lo and Ld phases of the ternary membranes (panel e). The five ternary systems are given in Fig. 2a, 2b, and 2d. Plotted are the highest liquid-liquid demixing temperature (T_{mix}) of the ternary systems versus (a) the difference in the number of carbons in the two PC-lipid tails, (b) the highest single-component lipid gel-to-liquid melting temperature (T_{melt}), (c) the difference in thicknesses of single-component PC-lipid membranes ($d_{high} - d_{low}$), (d) the difference in

T_{melt} of single-component PC-lipid membranes ($T_{high} - T_{low}$), or (e) the estimated thickness difference between Lo and Ld phases of the ternary membranes. Numerical values are compiled in Table 1 and Table S1.

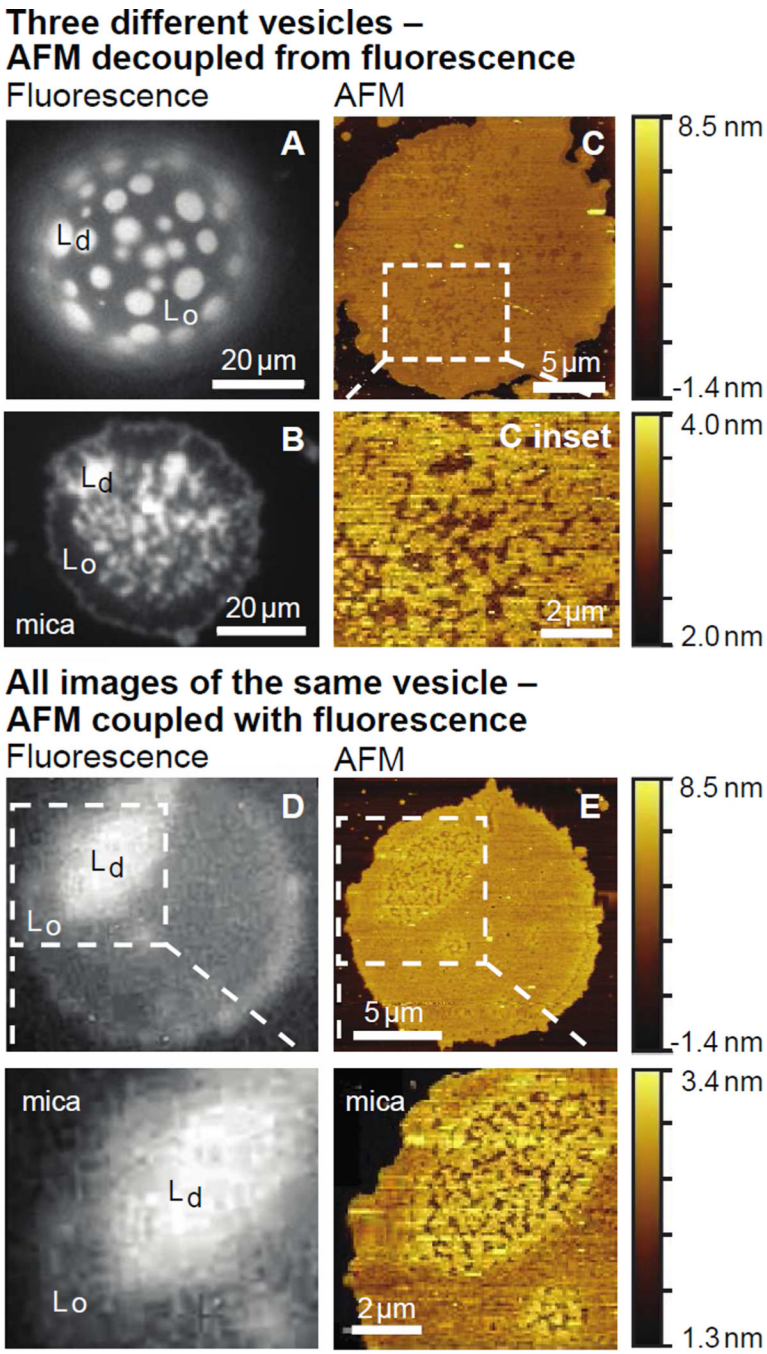

Figure 4.

Room temperature fluorescence microscopy (left) and AFM topography (right) of membranes composed of 20/40/40 mol% 4Me-16:0-PC/13:0-PC/chol (top) and 20/55/25 mol% 22:1-PC/16:0-PC/chol (bottom). All membranes contain 0.8 mol% Texas Red DHPE. (A) Fluorescence microscopy image of a giant unilamellar vesicle (GUV) and (B) an isolated supported lipid bilayer formed by rupturing a GUV onto mica. (C) AFM topography of a different supported lipid bilayer made from the same lipid composition. (D)

Fluorescence microscopy image of a supported lipid bilayer. (E) AFM topography of the same region.

Table 1

Estimated thickness differences of Lo and Ld phase membranes; Phase behavior of ternary lipid membranes containing a low-T_{melt} lipid, a high-T_{melt} lipid, and cholesterol

low-T_{melt} lipid	high-T_{melt} lipid	Estimated $d_{Lo} - d_{Ld}$ (Å)[a]	PC-lipid $d_{high} - d_{low}$ (Å)[b]	Lo/Ld coexist ≥25°C[c]	Fig.[d]
4Me-16:0-PC	13:0-PC	1.9	−0.7[e]	Yes	2a
20:1-PC	16:0-PC	−0.7	−3.5	Yes	2a
22:1-PC	16:0-PC	−4.3	−7.4	Yes[f]	2a
4Me-16:0-PC	12:0-PC	0.1	−2.8	No	2b
20:1-PC	14:0-PC	−4.5	−5.8	No	2b
22:1-PC	17:0-PC	−2.6	−5.8[e]	No	2c
24:1-PC	16:0-PC	−7.9	−13.2	No	2c
24:1-PC	18:0-PC	−3.7	−10.0	No	2c

[a] Estimates of thickness differences between Lo and Ld phases in ternary membranes of the high-T_{melt} lipid, the low-T_{melt} lipid, and cholesterol, using assumptions from incomplete literature sources. Derivations and uncertainties of estimates are described in the Methods.

[b] Difference in membrane thickness between single component membranes comprised of the high-T_{melt} (d_{high}) and low-T_{melt} (d_{low}) lipids in liquid phases.[9–10]

[c] Whether or not the ternary system (with cholesterol) exhibits coexisting liquid phases above 25 °C.

[d] Location of phase diagrams in Fig. 2.

[e] Data estimated as an average of thicknesses of membranes comprised of lipids with tails containing one more and one fewer carbon.

[f] Requires exposure to light to undergo phase separation into Lo and Ld phases.

Table 2

Lo:Ld and Thick:Thin membrane area ratios, with measured thickness mismatches.

Ternary membrane[a] (mol %)	Lo:Ld area GUVs[b]	Lo:Ld area SLBs[c]	Thick:Thin area AFM[d]	Thickness Mismatch (Lo−Ld, Å)[e]
20:1-PC/16:0-PC/chol (20/60/20)	67:33 ± 2 (N = 23)[f]	78:22 ± 3 (N = 8)	73:27 ± 2 (N = 3)	9.6 ± 0.1 (N = 3)
20:1-PC/16:0-PC/chol (50/30/20)	24:76 ± 2 (N = 25)	25:75 ± 3 (N = 7)	32:68 ± 9 (N = 4)	8.3 ± 0.1 (N = 4)
4Me-16:0-PC/13:0-PC/chol (30/40/30)	43:57 ± 2 (N = 23)	43:57 ± 1 (N = 10)	40:60 ± 8 (N = 3)	3.3 ± 1.2 (N = 3)
4Me-16:0-PC/13:0-PC/chol (20/40/40)	64:36 ± 3 (N = 13)	69:31 ± 1 (N = 46)	75:25 ± 7 (N = 4)	5.9 ± 1.0 (N = 4)
22:1-PC/16:0-PC/chol (20/55/25)	– direct identification –			−4.4 (N = 1)

[a] All systems contain 0.8 mol% Texas Red DHPE.

[b] Ratio of Lo:Ld domain areas covering the surface of free floating giant unilamellar vesicles (GUVs), as determined by fluorescence microscopy.

[c] Ratio of Lo:Ld domain areas covering the surface of supported lipid bilayers (SLBs) made from ruptured GUVs, as determined by fluorescence microscopy.

[d] Ratio of SLB thick:thin domain areas determined by AFM.

[e] Thickness mismatch of Lo and Ld phases determined by AFM, and standard error of the mean.

[f] Number of vesicles measured.